

## Experience and Modeling of a Rotating Electrode for the Removal of Sand Particles on PV Panels

Miloud Kachi and Hana Bechkoura\*

Electrical engineering laboratory, University 8 May 1945, B.P.401, Guelma, 24000, Algeria

Received 23 July 2024; Accepted 29 January 2025

### Abstract

Photovoltaic (PV) stations installed in desert environments face different challenges, particularly from sandstorms that can lead to significant sand accumulation on the panels, which reduces their efficiency. This paper investigates a simple yet effective solution based on electrostatic induction to address this issue. The system consists of a stainless-steel cylindrical electrode rotating at 150 rpm, that moves above the glass surface to remove the accumulated sand. By inducing charges, the electric field attracts sand particles toward the electrode through electrostatic attraction, but once the particles make contact, they are repelled away from the electrode. The repulsion phenomenon, in conjunction with the centrifugal force, resulted in an enhanced orientation of the displaced particles. Both theoretical and experimental studies are conducted to examine the particle dynamics, particularly focusing on their behavior after being released by the electrode. Furthermore, the attraction distance of the electrode is calculated for different voltages and electrode diameters. Cleaning efficiency is experimentally evaluated by measuring the transparency of the treated glass through light intensity. Light is measured before and after cleaning, using a light sensor positioned beneath the glass. The cleaning efficiency is quantified by comparing the amount of light transmitted through the sand-covered glass before cleaning with the light transmitted after cleaning, relative to a new, clean glass. The results demonstrate a high sand removal efficiency, with over 95% recovery of the glass transparency after treatment. In addition, the increased amount of light after cleaning is measured for three voltages (10, 11, and 12 kV) and three distances (0.5, 1, and 1.5 cm) between the cylinder and the grounded plate. The results revealed an increase of up to 200% of light transmitted through the glass after the cleaning process compared to the light before. Furthermore, the induction electrode is power efficient since it absorbs only 3W at 12.4kV.

*Keywords:* electrostatic induction, rotating electrode, sand particles, PV panels, electrostatic cleaning.

### 1. Introduction

The fight against climate change has expedited the search for sustainable, renewable energy resources to replace conventional fossil fuels. Due to the amount of sunshine and available land, photovoltaic (PV) panels are one of the recommended solutions in large, arid areas like the Algerian Sahara. Unfortunately, the PV stations in these areas are exposed to sand winds that have the potential to completely cover the panels and prevent light from reaching the cells. This significantly lowers their productivity [1], [2] and requires cleaning in order to restore their efficiency. Over the years, solutions to this problem have been suggested starting from obvious to a more sophisticated one. Among them nano layer coating, water cleaning, rotating brush driven manually, mechanically, or even by a robot were suggested [3], [4]. Applying such cleaning methods to a large-scale PV power station installed in the desert would require a huge quantity of fresh water but also poses a logistic and power issues. Since then, water-based solutions or techniques with relatively high-power consumption should be avoided in arid areas. Alternatively, non-contact and dry methods have been developed, claiming to be more power and cost effective [5]. Electrostatic cleaning belongs to this class of dry and often non-contact methods that offer power and water savings along with a high efficiency. The electrostatic solutions are convenient to desert environment where climate is dry, with

high temperatures and low humidity. The basics of electrostatic methods can be categorized in three distinct principals: travelling, or standing wave of an electric curtain (electrodynamic), ionic wind from an electric discharge, and induction electrodes. Initially proposed for space application, the travelling wave electric curtain developed by Masuda [6], has no moving parts, and has extremely low energy consumption [5]. This type of electric curtain is formed by a set of polyphasic parallel electrodes fed through at least a three-phase system, similar to a three-phase electric motor. The polyphase nature of this system and the complexity of the electrode connection led to the development of another one-phase or biphasic configurations of the electric curtain [7]. These versions necessitate fewer power sources but generate a standing or pulsating wave rather than a travelling electric wave. The created standing wave repels and moves particles through the simultaneous action of various electric and non-electric forces. To be effective, the curtain has to be embedded in the surface to be cleaned. This creates a problem of applicability on a large-scale station as well as efficiency reduction due to the light inhibition by the electrodes themselves. A similar approach was lately proposed, which consists of installing a mesh of electrodes above the panels and connecting it to an HV source powered by a wind-driven rotary electret generator [8]. Another electrostatic approach uses ionic wind generated by a moving corona electrode [9]. The method is quite simple, since it uses a thin electrode subject to a high voltage of around 25 kV placed near a grounded frame. The generated ionic wind reaches 2 m/sec

\*E-mail address: hana.benchkoura@gmail.com

ISSN: 1791-2377 © 2025 School of Science, DUTH. All rights reserved.

doi:10.25103/jestr.181.08

and was able to clean until 95% of deposited sand. However, the dependence of the corona discharge on environmental conditions such as temperature and humidity [10], besides the need for a relative higher voltage (25 kV) and the generated ozone gas in the surrounding areas, could be a downside of this technique. In addition to the above methods, an easier electrostatic way to repel sand particles consists of using the electric induction principle [11]. This method utilizes a simple metallic plate electrode connected to an HV power supply and suspended at a distance while moving along the surface. In this method, the electric field from the plate acts like a blower where sand particles are attracted or repelled in all possible directions. This way, rejected particles can be pushed towards the already cleaned surface. Therefore, the induction plate electrode suffers from the lack of control of particles direction.

In this paper, the electrostatic induction principal is applied to clean the surface of a glass covered by a sand quantity. For this purpose, a rotating cylindrical electrode connected to HV source moves over the glass and attracts the sand particles through electric forces. The proposed approach has the ability to push attracted particles in one direction thanks to the rejected particles through both centrifugal and repulsion forces. This design result in a more consistent cleaning and better control of particle direction. The presented design relies on a conductive cylinder connected to HV and suspended above the panels. This simple principal can therefore easily be applied even for large-scale stations. Since humidity is low in the desert environment, this electrostatic solution is expected to work without issues.

## 2. Materials and Methods

Fig. 1 illustrates the basic concept of the applied induction method. The induction electrode is a cylindrical metallic electrode made of stainless steel of 5 cm diameter suspended at 1 cm above the surface of a glass to be cleaned. The electrode is rotating at a speed of around 150 rpm while moving horizontally at roughly 0.8 cm/sec. The maximum speed values are imposed by the mechanical parts of the translation and rotation mechanisms. Both, translation motor (carrying the system) and the motor driving the cylinder have a mechanical reduction that limit their maximum speed. In all experiments the electrode was connected to a positive DC high voltage power supply. The measurements were conducted under ambient conditions during two different months: June and December, with temperatures and humidity levels of 33°C and 40%, and 12.6°C and 61.8%, respectively. The DC high-voltage power supply is limited to 12 kV, so in our experiments, the maximum voltage typically used is below 12 kV—often 11 kV—unless otherwise specified. Another limiting factor in our experiments is the occurrence of parasitic discharges in the developed lab prototype, which can alter the voltage and, consequently, impact the performance of the cleaner. A quantity of the desert sand is uniformly deposited on the glass and then passed under the rotating electrode. The performances of the method was evaluated by measuring light intensity passing through the glass before and after cleaning. A light sensor is placed under the glass to record the light intensity while a fixed lamp illuminates the upper surface (Figure 1.b). This light measurement is carried out along the central axis of the glass while it moves at a fixed speed.

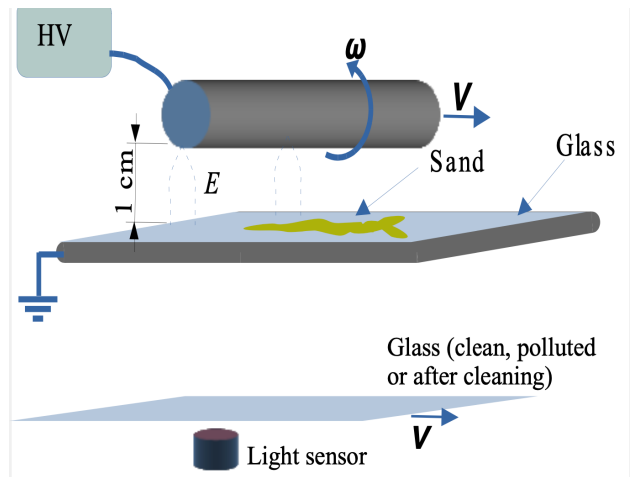


Fig. 1. Experimental setup: (a) Rotating induction electrode - up, and (b) light measurement for efficiency evaluation-down.

## 3. Theoretical aspect

### 3.1. Computation of the electric field

Fig. 2 shows a schematic representation of the cylindrical electrode for the calculation of the electric field and particle trajectory. Due to the symmetry, only half of the configuration is studied.

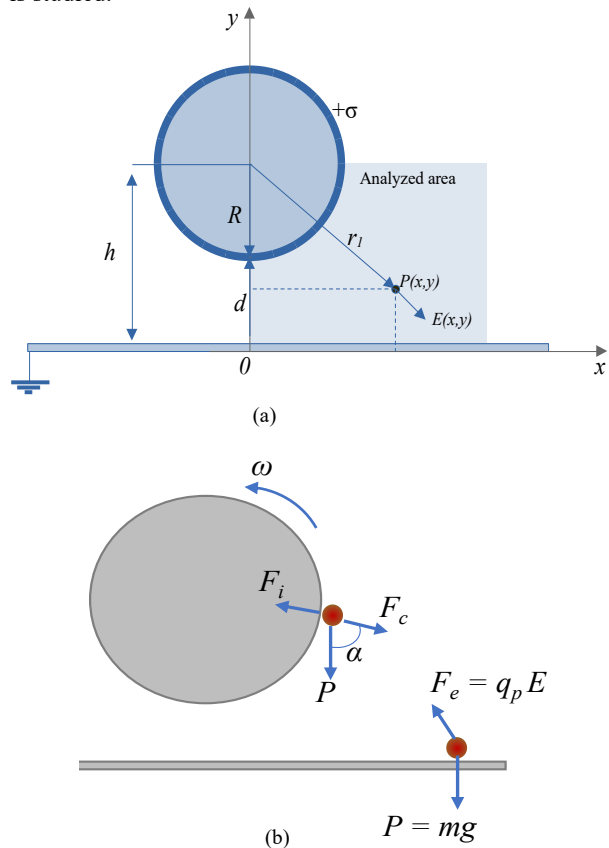


Fig. 2. Calculation of the electric field distribution due to the cylindrical electrode above the grounded plate.

The electric field in the air gap between the energized cylinder and the grounded metallic plate is determined using the method of images. Therefore, at a point  $P(x,y)$  situated at " $r_l$ " distance from the center of the cylinder, the electric field is the sum of the two electric fields generated by the real and

the fictive cylinder. Gauss theorem applied to the real cylinder gives:  $E_1 = \frac{Q_1}{2\pi\epsilon r_1 L}$ . In the same way, the electric field created by the fictive cylinder is:  $E_2 = \frac{Q_2}{2\pi\epsilon r_2 L}$ , where  $r_1$  and  $r_2$  are the distances from the center of the cylinder until the point  $P(x,y)$  for the real and the image cylinder respectively. These distances are given by:

$$r_1 = \sqrt{(x^2 + (y - h)^2)}$$

$$r_2 = \sqrt{(x^2 + (y + h)^2)} \quad (1)$$

Summation of  $E_1$  and  $E_2$  would result in the total field  $E$  with components on  $x$  and  $y$  axis  $E_x$  and  $E_y$  given by [12]:

$$E_x = \frac{\sigma x R}{\epsilon_0} \left[ \frac{1}{r_1^2} - \frac{1}{r_2^2} \right]$$

$$E_y = \frac{\sigma R}{\epsilon_0} \left[ \frac{y-h}{r_1^2} - \frac{y+h}{r_2^2} \right] \quad (2)$$

The magnitude of the total electric field is then:

$$E = \sqrt{E_x^2 + E_y^2}$$

The charge density  $\sigma$  on the surface of the metallic cylinder can be obtained from the minimum distance between the cylinder and the grounded plate where  $y = d$  and  $x = 0$  (Fig. 2). At that point,  $E_x = 0$ , and  $E_y = U/d$ . Applying these conditions to equations (1) and (2) yields the surface charge density on the electrode:

$$\sigma = \frac{U \epsilon_0}{d R} \frac{1}{\left[ \frac{1}{R^2} + \frac{1}{d+h} \right]} \quad (3)$$

The electric field was also calculated using finite element method using FEMM software [13]. The electric field distribution on the grounded plate obtained analytically and numerically were compared. The movement of the particle is then studied based on the comparison results.

### 3.2. Charge and forces on a sand particle in a non-ionized electric field

Inductively charged particle placed on a grounded plate crossing an electric field is subject to forces that tend to levitate and move the particle toward the energized electrode, whereas other forces tend to keep the particle on the plate. Sand particles with 200  $\mu\text{m}$  – 400  $\mu\text{m}$  size [6], are big enough to neglect the adhesion force (Van der Waals) and only consider their weight. In this case, the lift-off condition would be:

$$F_e > P \quad (4)$$

Where  $P = \rho \cdot vol \cdot g$  is the particle's weight,  $\rho = 1850 \text{ kg/m}^3$  the density and  $vol$  is the volume of the particle ( $vol = \frac{4}{3} \pi R_p^3$ ).  $F_e$  is the electric force exerted by the electric field on the particle on the grounded plate given by [14], [15]:

$$F_e = 0.832 Q_p E(x, y) \quad (5)$$

movement of the particle will, therefore, result from the imbalance between the applied electrical and mechanical

forces. A key factor in this interaction is the electric charge induced on the conducting or quasi conducting particle, which depends on the electric field. Assuming a spherical particle of radius  $R_p$  situated at  $(x,y)$  position, the induced electric charge is given by [14], [16]:

$$Q_p = \frac{2}{3} \pi^3 \epsilon R_p^2 E(x, y) \quad (6)$$

$R_p$  is the particle's radius taken 300  $\mu\text{m}$  during calculation.  $E(x,y)$  is the electric field at  $x$  and  $y$  position.

As the particle lifts off and move towards the cylindrical electrode, the value of the induced charge on the particle will vary according to its position. When it reaches the electrode, the charge of the particle changes suddenly to a new value that depends on the conductivity of the particle. Indeed, sand with poor conductivity and polarizability aptitude ( $\epsilon_r > 1$ ) [17], [18], that depend on humidity, can show various behaviors when in contact with the energized metallic electrode. If the particle is considered highly conductive, it will immediately be at the same voltage, and polarity, as it touches the electrode and, therefore, will be rejected back through repulsion force. In this case, since both potentials are equal  $V_p = V_c$ , the surface charge density on the particle relative to the cylindrical electrode would be:

$$\sigma_p = \sigma_c \frac{R_c}{R_p} \quad (7)$$

Where  $\sigma_p$  refers to the charge density of the particle density and  $\sigma_c$  to the charge of the cylinder, given by (3). But, in case of slightly insulating behavior, the particle can retain a charge and remain attached to the electrode through image force [16]:

$$F_i = \frac{Q_p^2}{4\pi\epsilon_0(2R_p)^2} \quad (8)$$

The particle leaves the electrode if the image force is lower than the sum of centrifugal force and particle's weight as shown in Fig. 2.b:  $F_i < F_c + P \cos(\alpha)$ .

In the air, during the attraction phase, after the lift-off, or after the detachment from the electrode, the particle is facing a drag force due to the surrounding air:

$$F_{dx,y} = -\frac{1}{2} C_d \rho_{air} S_p V_{x,y}^2 \quad (9)$$

Where  $C_d = 0.47$  is the drag coefficient,  $\rho_{air} = 1.225 \text{ kg/m}^3$  is the air density,  $S_p$  is the particle's surface, and  $V_{x,y}$  the speed in  $x$  and  $y$  direction.

### 3.3. The trajectory of the particle

When the particle is not in contact with the cylindrical electrode, the movement is governed by the following equations:

$$\frac{dx}{dt} = V_x$$

$$\frac{dV_x}{dt} = \frac{(-F_{ex} + F_{dx})}{m}$$

$$\frac{dy}{dt} = V_y$$

$$\frac{dV_y}{dt} = \frac{(F_{ey} + F_{dy} - P)}{m} \quad (10)$$

As soon as it touches the electrode, its speed and position are imposed by the speed and position of the rotating electrode itself. When released, the particle would have the initial speed  $V_t = \omega R$ .

#### 4. Results and Discussion

Modelling results are presented in section 4.1, whereas, the other sections are devoted to the experimental measurements.

##### 4.1 Modelling results

Fig. 3 shows the calculated distribution of the electric field. Figure 3.a illustrates the distribution and streamlines of the electric field as determined by the analytical model, while fig. 3.b compares the electric field values at the grounded electrode, obtained from both analytical and numerical calculations. As shown in fig. 3.b, the analytical method can reasonably predict good values just under the electrode, at the minimum distance ( $x = 0$ ), but as the distance increases, the analytical model overestimates the electric field intensity in comparison to the finite element model, implemented in FEMM software. Since the electric field intensity and the charge of the particle are the main components that control the overall behavior of the particle, the movement is studied using both models.

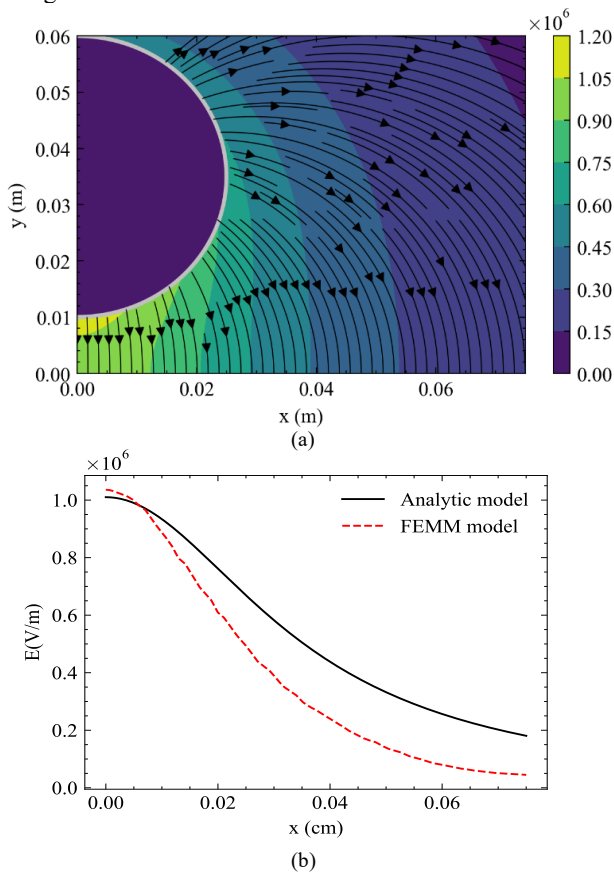


**Fig. 3.** Electric field distribution (V/m) at 11 kV and 1 cm distance between electrodes: (a) intensity and stream lines, and (b) comparison of the electric field values at the level of the grounded plate.

Fig. 4 depicts the trajectory of the particle for three possible situations of the charge on the particle after being released from the electrode: positive, negative, and zero. If the particle in the air has a zero charge, it would behave as a simple mass thrown with an initial speed  $V_t$  and therefore would fall on the grounded electrode due to gravity and air

resistance. When the charge is negative, the centrifugal force and the weight can detach it from the electrode, but it is attracted again by the electric field, which creates an oscillation movement near the surface of the electrode. However, despite the oscillation, the particle still continues its rotation along with the electrode. Finally, when the charge is positive, the particle is immediately rejected by the electrode to fall over the grounded plane. This latter case is probably the most observed behavior. Therefore, the charge, which depends on the properties of the sand particle, will define its behavior. It is expected that two charging mechanisms are involved: induction for levitation, and contact charging after the particle reaches the electrode. When released in the air, it can be subject again to the induction phenomenon. The practical situation is more complex as the electrode continuously attracts many particles at the same time. In this case, there is an interaction and collision between particles near the surface of the electrode and in space between the electrode and the plane. This case is difficult to simulate as it involves many secondary phenomena, such as electrostatic interaction between a lot of particles with or without the same charge, in addition to the mechanical collision between them. This case requires a more detailed simulation and hence more resources, which is indeed beyond the scope of this paper.

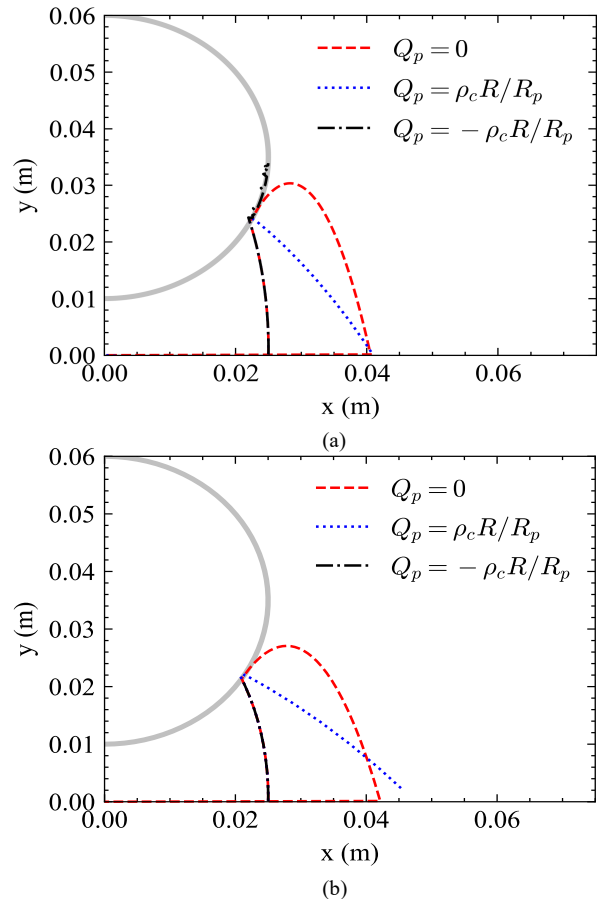


**Fig. 4.** Particle trajectory at 11 kV for three charges situations after the particle leaves the electrode:  $Q_p < 0$ ,  $Q_p = 0$  and  $Q_p > 0$ . The initial conditions where  $x_0 = R$ ,  $V_x = 0.8$  cm/s,  $y_0 = R_p$ ,  $V_y = 0$ . The trajectories are calculated using electric field distribution obtained by (a) analytical, and (b) numerical models.

The movement of the particle is not really affected by the model used in calculating the electric field. For the same conditions, both numerically and analytically calculated electric fields bring a close result in terms of the particle trajectories, as shown in Fig. 4.a and Fig. 4.b. Because the

numerical model predicts less intensity of the electric field far from the center of the electrode, the detached particles from the cylinder travel more distance of a few millimeters before failing over the grounded plate.

The electrode attraction capability depends not only on the applied voltage but also on the dimensions of the electrode, as represented in Fig. 5. Overall, the attraction distance, counted from the center of the electrode, increases almost linearly with the voltage  $x_{lim} = k.U.$ , where  $k$  is the slope of the curve. The slope increases in turn when the electrode radius increases. Therefore, the bigger the electrode, the better the attraction capability. However, increasing the electrode diameter means increasing weight. Hence, a compromise should be reached between these two parameters.

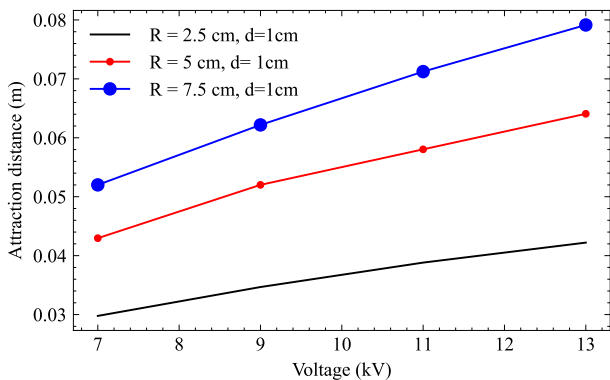


Fig. 5. Attraction distance as function of the voltage and the radius of electrode. The distance is counted from the center of the electrode.

#### 4.2 Experimental measurements of the cleaning efficiency

The cleaning efficiency was calculated based on the amount of light that passed through the transparent glass. For this experiment, a clean glass surface measuring 8 cm by 4.5 cm was uniformly covered with 1 gram of sand from the Algerian desert, as shown in Fig. 6.a. Light intensity was measured along the center of the sand-covered area, with a light sensor placed directly beneath the contaminated glass. As illustrated in Fig. 6.b, the sand-covered glass was then cleaned by passing it beneath a rotating electrode. Following the cleaning process, the transparency of the glass was re-evaluated using the same method as before, as shown in Fig. 6.c. By comparing the light intensity passing through the glass before and after cleaning, the cleaning efficiency can be calculated as the ratio:  $\frac{Light_{after}}{Light_{clean}} 100\%$ .

Fig. 7.a represents the results of the light measurements for a clean transparent glass, the polluted glass with sand, and the glass after cleaning. It is obvious that pollution decreases the light intensity by nearly half compared to clean glass. After cleaning, the glass transparency is restored to an acceptable value. Fig. 7.b shows the cleaning efficiency measured by comparing light after cleaning to a clean glass along the surface. As can be seen, the efficiency exceeds 90% on most of the cleaned surfaces and can reach 96% transparency compared to a clean glass. Although most of the sand was removed, there is still a residual small quantity, essentially formed by fine particles that have a higher adherence force. The influence of this residual fine particles is negligible as light can massively reach the PV cells. However, the optimization of the system could resolve a major part of these residual small quantities. This includes a

compromise between various parameters: voltage, distance, radius, rotation, and so on.

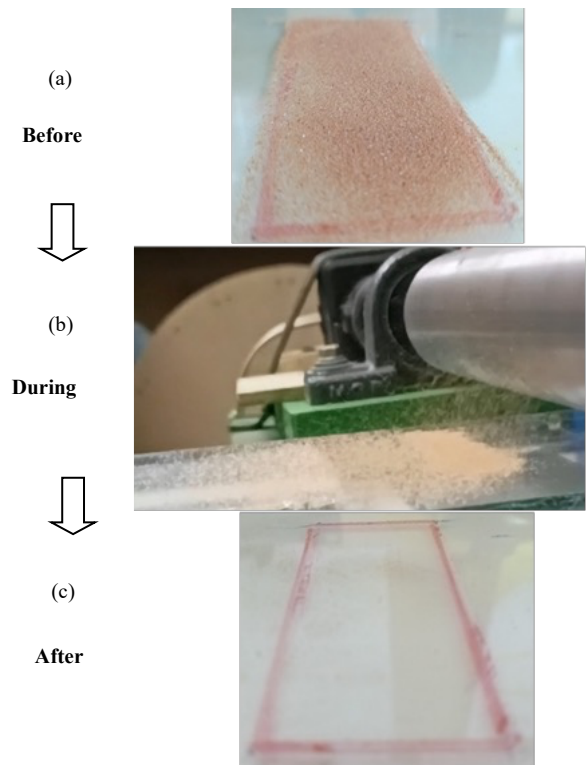


Fig. 6. Cleaning operation using the rotating electrode of 2.5cm radius and 11 kV voltage (distance from the upper surface around 1 cm): (a). before cleaning, (b) during cleaning, and (c) after cleaning.

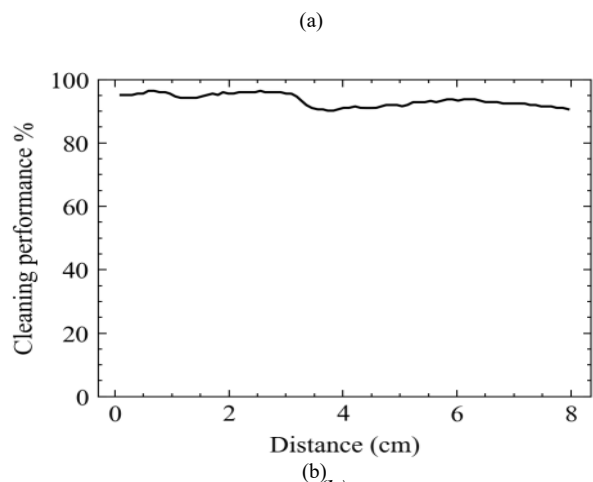
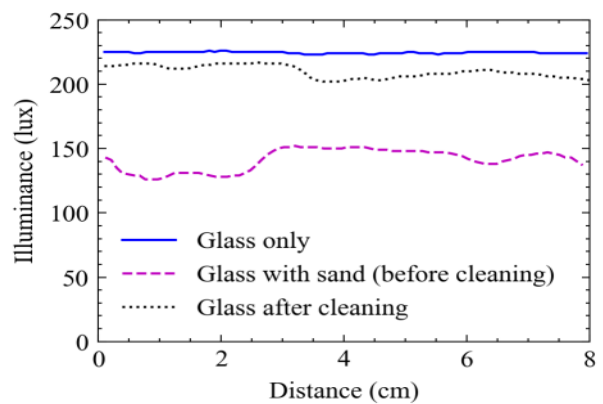


Fig. 7. Cleaning performance measurements using light transparency: (a) light through clean glass, polluted glass and after cleaning, and (b) ratio of light after cleaning by light of a clean glass.

### 4.3. Influence of the electrode 'rotation

To show the importance of the electrode rotation, a cleaning experience was realized without rotation of the electrode.

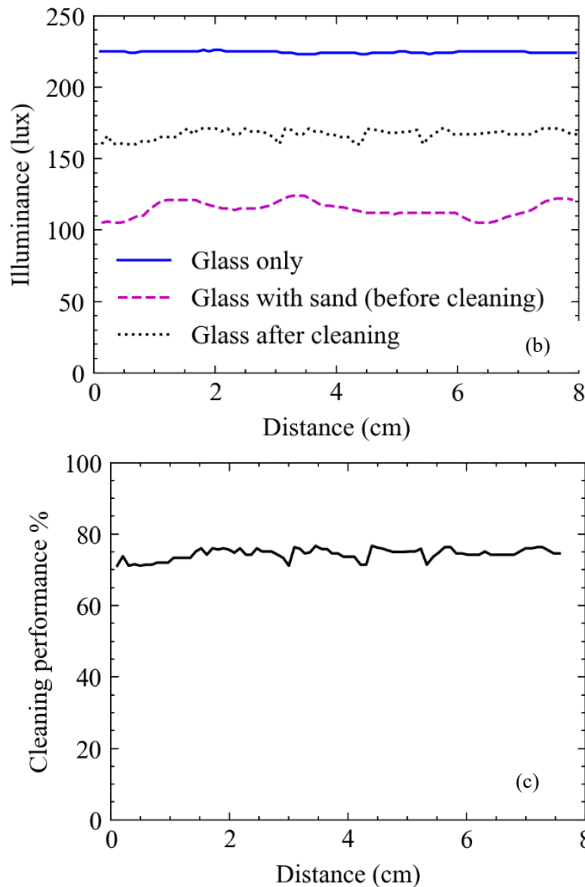


Fig. 8. Results of non-rotating electrode: (a) photography, (b) Light measurements for transparency results for a non-rotating electrode, and (c) cleaning efficiency.

In this case, the polluted glass was scanned by the electrode without any rotation. As expected, the particles are attracted and repelled in the surrounding area including the zone already cleaned, as shows the Fig. 8. Therefore, the centrifugal force plays an important role in the displacement of the particle in one direction.

Fig. 8 shows the light measurement results for the electrode without rotation. Indeed, because the repelled particles are thrown in all directions, the particles are left behind the electrode in the zone already cleaned. Without rotation, the process performance was less than 80%, compared to more than 95% with rotation. It can be easily shown that the rotation movement increases the cleaning efficiency by more than 15%.

### 4.4. Influence of the voltage and the distance between electrode on the quantity of removed sand

In these experiences the removed quantity of sand was evaluated based on light measurements before and after cleaning. The ratio of light after on light before cleaning ( $\frac{light_{after}}{light_{before}} \cdot 100\%$ ) shows the increased amount of light due to the sand removal. So, this ratio indirectly refers to the estimation of the removed sand quantity. This ratio is studied for three voltages 10 kV, 11 kV and 12 kV and three distances between the cylinder and the grounded plate 0.5 cm, 1cm, and 1.5cm.

#### 4.4.1. Influence of the voltage

Fig. 9 shows the mean values of the ratio of light after on light before, measured for three voltages. The results are medium values of three measurements. After cleaning, the amount of light increases by 125% to 150% at 10 kV and reaches 175% to 200% at 12 kV, compared to the light before cleaning. This means that increasing the voltage drastically improves the cleaning efficiency and hence the removed sand quantity. The more the voltage, the better the cleaning. It is easy to justify this voltage influence because it is directly related to the intensity of the electric field. As the voltage increases, the electric field increases as well, leading to higher attraction forces. Therefore, the removal of sand is improved when the voltage is increased.

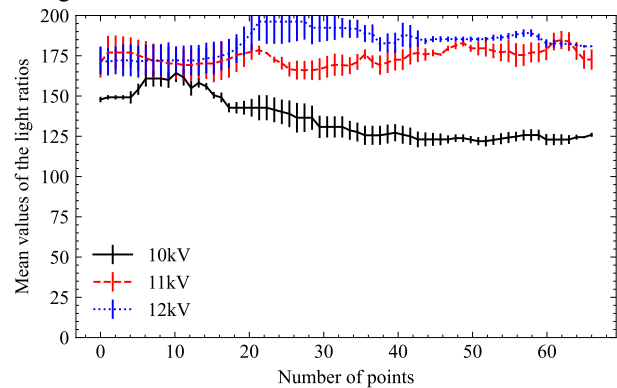


Fig. 9. Mean values of the light ratio ( $light_{after}/light_{before}$ ) as function of the distance for three voltages. The error bars show the standard deviation calculated for three experiences.

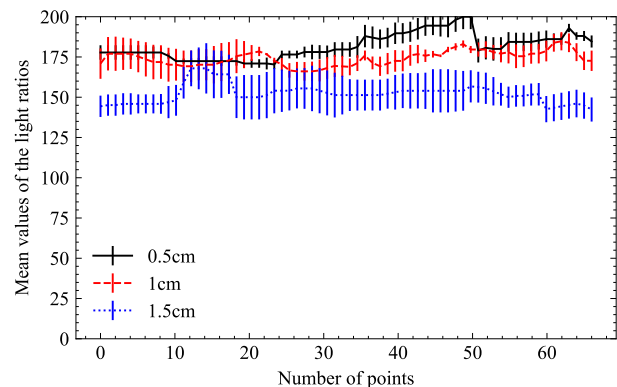


Fig.10. Variation of the mean values of light ratio as function of the distance between the cylinder and the grounded electrode (11 kV). Error bars show standard deviation values for three experiences.

#### 4.4.2. Influence of the distance

Fig. 10 illustrates the influence of the distance between the cylinder and the grounded electrode on the increased amount of light after cleaning at 11 kV. This result shows that decreasing the distance increases the removal of sand

particles and hence increases light after the cleaning process. This is due to the increase of the electric field in the air. Indeed, as the distance between electrodes decreases, the electric field between electrodes increases, which in turn increases the attraction forces between the sand particles and the rotating electrode.

#### 4.5. Washed glass measurements

For comparison purpose, the light was measured in the case of cleaned glass with fresh water. Fig. 11 shows the obtained results for water cleaning method case, before and after cleaning. The measurements were carried out just after cleaning, when the glass is still wet, and after the drying the glass. It is interesting to show that water droplets can alter the transmitted light through diffraction phenomenon. Indeed, the water droplets have the ability to concentrate the light by playing the same role as lenses. For that reason, the light after cleaning exceeds the reference curves in some places. Overall, the method delivers a good performance and can recover almost all the glass transparency.

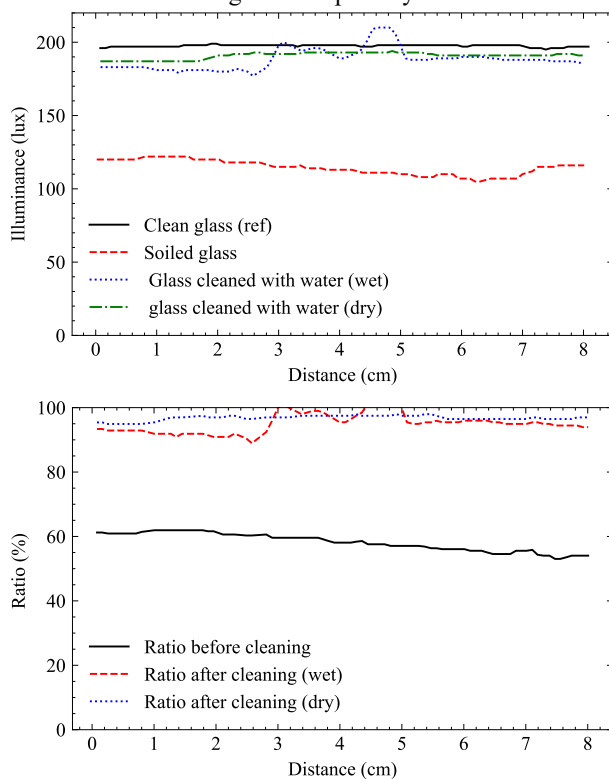


Fig. 11. Glass cleaned with water: Light values for clean, soiled, and water cleaned glass just after cleaning (wet) and after a drying (dry). At the bottom, the ratio of light before and after cleaning to the clean glass (Reference curve).

#### 4.6. Energy consumption of the rotating induction electrode

The consumed currents are measured for each part of the system. The results are summarized in Table. 1. Noting that existing parasitic discharge increases the absorbed current by the electrode. As shown by these power consumption results, the device is very efficient and absorbs a very low amount of power that varies according to the applied voltage. At the maximum reached voltage of 12.37kV, the absorbed power is about 3W only, which is a very low amount of power. On the

other side, the motors that rotate the cylinder and move the conveyor have almost identical consumption of 20 W. If the design is changed to include a mechanical conversion of the movement, it is possible to reduce the number of motors to only one. The total system absorbs about 44 W, despite the fact that it is not optimized and employs heavy metals, like stainless steel. Relatively to 300W panels, this represents 14.6% of the produced power. Considering the system is working only when the light is drastically reduced, the consumed power over time (energy) is almost negligible.

Table 1. Power consumption of the system

Part	Current	Voltage	Power
Metallic cylinder	0.087mA	7kV	0.609 W
	0.164mA	10kV	1.64 W
	0.198mA	11kV	2.17 W
	0.240mA	12.37kV	2.968 W
Motor 1	0.11A	220V	21 W
Motor 2	0.10 A	220V	20 W

#### 5. Conclusion

A rotating induction electrode as a simple electrostatic solution to clean the surface of PV panels in a desert has been theoretically and experimentally studied. The study pointed out the following results:

- From the theoretical model, it is inferred that attraction distance of a cylindrical electrode increases with the increase of the diameter of the electrode and the applied voltage.
- The glass transparency was evaluated through measurement of the light crossing the glass in three states: clean, polluted, and after being cleaned by the electrode.
- The experience showed the good cleaning capability of the rotating induction electrode, since more than 95% of the initial transparency was recovered after cleaning.
- The rotation movement is crucial for the displacement of the particles in one direction and avoiding their dispersion in all direction around the electrode.
- The applied voltage and the distance between the energized electrode and the grounded surface both enhance the removal efficiency. Higher voltage improves performance, while a shorter distance between the electrodes leads to better cleaning results.
- The induction electrode is very efficient in terms of consumed power. It absorbs a current of 0.24mA at 12.3kV, leading to around 3W of power.
- The optimization of the system is required to achieve better results.

This is an Open Access article distributed under the terms of the Creative Commons Attribution License.



#### References

[1] W. J. Jamil, H. Abdul Rahman, S. Shaari, and Z. Salam, "Performance degradation of photovoltaic power system: Review on mitigation methods," *Renew. Sustain. Ener. Rev.*, vol. 67, pp. 876–891, Jan. 2017, doi: 10.1016/j.rser.2016.09.072.

- [2] F. Mohammadi, A. Hajinezhad, A. Kasaecian, and S. F. Moosavian, "Effect of Dust Accumulation on Performance of the Photovoltaic Panels in Different Climate Zones," *Int. J. Sustain. Ener. Environm. Res.*, vol. 11, no. 1, pp. 43–56, Jun. 2022, doi: 10.18488/13.v11i1.3041.
- [3] J. Farrokhi Derakhshandeh, R. AlLuqman, S. Mohammad, H. AlHussain, G. AlHendi, D. AlEid, et al. "A comprehensive review of automatic cleaning systems of solar panels". *Sustain. Energy Technol. Assessments*, vol.47, August 2021, Art. no. 101518.
- [4] A. Chadly, H. Y. Aldayyani, M. M. Hamasha, S. Amer, M. Maalouf, and A. Mayyas. "Selection of optimal strategy for managing decentralized solar PV systems considering uncertain weather conditions." *Sci. Rep.*, vol. 14, May 2024, Art. no. 12269.
- [5] H. Kawamoto and B. Guo. "Improvement of an electrostatic cleaning system for removal of dust from solar panels". *J. Electrostat.*, vol. 91, pp. 28–33, Feb. 2018.
- [6] S. Masuda, K. Fujibayashi, K. Ishida, and H. Inaba. "Confinement and Transport of Charged Aerosol Clouds by Means of Electric Curtains". *Trans. Inst. Elec. Eng. of Japan B*, vol. 92, no. 1, pp. 9–18, Jan. 1972.
- [7] H. Bechkoura, N. Zouzou, and M. Kachi. "Mechanics of Particle Motion in a Standing Wave Electric Curtain: A Numerical Study". *J. Atm.* vol. 14, no. 4, Apr. 2023, Art. no. 681.
- [8] R. Ding, Z. Cao, J. Teng, Y. Cao, X. Qian, W. Yue, et al. "Self-Powered Autonomous Electrostatic Dust Removal for Solar Panels by an Electret Generator." *Adv. Sci.*, vol. 11, no. 26, Jul. 2024, Art. no. 2401689.
- [9] A. Tilmatine, N. Kadous, K. Yanallah, Y. Bellebna, Z. Bendaoudi, and A. Zouaghi. "Experimental investigation of a new solar panels cleaning system using ionic wind produced by corona discharge". *J. Electrostat.* vol. 124, Jul. 2023, Art. no. 103827.
- [10] J. Qu *et al.*, "A review on recent advances and challenges of ionic wind produced by corona discharges with practical applications," *J. Phys. D: Appl. Phys.*, vol. 55, no. 15, Apr. 2022, Art. no. 153002, doi: 10.1088/1361-6463/ac3e2c.
- [11] S. Panat and K. K. Varanasi, "Electrostatic dust removal using adsorbed moisture–assisted charge induction for sustainable operation of solar panels," *Sci. Adv.*, vol. 8, no. 10, Mar. 2022, Art. no. eabm0078, doi: 10.1126/sciadv.abm0078.
- [12] N. Ida, *Engineering Electromagnetics*. Cham: Springer International Publishing, 2021. doi: 10.1007/978-3-030-15557-5.
- [13] D. Meeker. "Finite Element Method Magnetics (FEMM)." Version 4.2, 2018. [Online]. Available: <http://www.femm.info/>. [Accessed: Dec. 30, 2024]
- [14] L. Dascalescu, S. Das, and U. Kumar, "Numerical simulation of conductive particle behaviour at the surface of a plate electrode affected by a DC corona field," *J. Electrostat.*, vol. 67, no. 2–3, pp. 167–172, May 2009, doi: 10.1016/j.jelstat.2008.11.010.
- [15] L. Dascalescu, A. Samuila, and R. Tobazéon, "Cylindrical conductive particles in the proximity of an electrode affected by a high-intensity electric field," *J. Electrostat.*, vol. 37, no. 3, pp. 173–196, Jul. 1996, doi: 10.1016/0304-3886(96)00011-3.
- [16] L. Dascalescu *et al.*, "Charges and forces on conductive particles in roll-type corona-electrostatic separators," *IEEE Trans. on Ind. Applicat.*, vol. 31, no. 5, pp. 947–956, Oct. 1995, doi: 10.1109/28.464503.
- [17] V. Guihard, J.-L. Adia, F. Lavergne, J. Sanahuja, and J. P. Balayssac, "Assessing the permittivity of an unsaturated sand by combining a Lattice Boltzmann Method simulation, electromagnetic homogenization models and measurements," *J. Appl. Geoph.*, vol. 173, Feb. 2020, Art. no. 103940, doi: 10.1016/j.jappgeo.2020.103940.
- [18] B. R. Vishvakarma and C. S. Rai, "Measurement of complex dielectric constant of sand and dust particles as a function of moisture content," in *23rd European Microw. Conf., 1993*, Madrid, Spain: IEEE, Oct. 1993, pp. 568–570. doi: 10.1109/EUMA.1993.336630.